23rd ABCM International Congress of Mechanical Engineering
December 6-11, 2015, Rio de Janeiro, RJ, Brazil

COMPUTATIONAL STUDIES OF FREE SURFACE FLOW BEHAVIOR FOR NEMATIC LCPS IN INJECTION MOULDING PROCESS

Pedro Alexandre da Cruz
Universidade Federal do Tocantins - Gurupi - Brasil
pedrocruz@uft.edu.br

Murilo F. Tomé
Universidade de São Paulo - São Carlos - Brasil
murilo@icmc.usp.br

Abstract. *This paper employs numerical approaches to investigate two-dimensional container filling with nematic LCPs fluids. For this, we present an efficient finite difference method to solve the free surface flow for nematic LCPs governed by the Ericksen-Leslie dynamic equations in container filling processes. The numerical technique is based on a projection method and solves the governing equations using primitive variables for velocity, pressure, extra-stress tensor and director. These equations are nonlinear partial differential equations consisting of the mass conservation equation and the balance laws of linear and angular momentum. We provide verification of the numerical code by comparing the numerical solutions obtained on several refined meshes. Convergence results are presented. Numerical results obtained for container filling employing LCPs are discussed.*

Keywords: *Free-surface flows, Ericksen-Leslie model, Container filling process, Nematic liquid crystal, Finite difference.*

1. INTRODUCTION

Nematic liquid crystalline polymers (LCPs) are anisotropic materials that have a wide range of applications in industrial processes (Bird *et al.*, 1987; Rey and Denn, 2002). When nematic liquid crystalline polymers are used in industrial products, the molecular orientation inside the products is important because of the characteristics of the liquid crystalline polymers highly depend on it. In polymer processing such as injection molding and container filling, molecules of LCPs are easily aligned by the flow and keep the alignment until solidification. The material properties of the nematic LCPs are then strongly affected by the flow processing. The injected polymer flows through the sprue and gate to the cavity. The fluid flow in moulded channels depends on many factors, like the properties of the polymer used, processing conditions and injection mould design. To obtain molded parts with expected properties, shape and surface, the flow can be controlled by the design, the mold technology and the processing conditions. The cavity in the injection mould should be filled totally during the injection phase and the filling should be laminar (Smorawinski, 1989; Beaumont *et al.*, 2002; Bociaga, 2001). During the entire process of injection molding and container filling various rheological phenomena may occur. These phenomena must be known and studied due to economic reasons, such as decrease in material waste and the need of shortening the injection cycle time, as well as the quality requirements for the moulded parts. Thus, the researches on experimental and numerical simulation to study phenomena that can occur during the flow of nemactic LCPs in injection molds and container filling are of valuable importance (Gonnet *et al.*, 2002). Many codes have been developed for analyze nematic LCPs flows (filling and other processes) with simplifications of the governing equations. This paper is concerned with the development of a finite difference algorithm capable of efficiently solving complex free surface flows using the complete Ericksen-Leslie model. The methodology developed extends previous works (see Cruz *et al.* (2010) and Cruz *et al.* (2013)), where confined nematic liquid crystal flows subject to a magnetic field were dealt with.

2. MATHEMATICAL MODELING

2.1 Governing Equations

The basic equations for two-dimensional flows of a nematic liquid crystal are the mass conservation equation, the elastic energy density, the linear and angular momentum equations which can be written, respectively, in dimensionless form as (for details see (Cruz *et al.*, 2011))

$$u_{,x} \;+\; v_{,y} = 0\,, \tag{1}$$

$$w_F \;=\; \frac{1}{2}\frac{1}{Re}\frac{1}{Er}\left[(\phi_{,x})^2 + (\phi_{,y})^2\right]. \tag{2}$$

$$u_t \;+\; uu_{,x} + vu_{,y} = -p_{,x} - w_{F,x} + R_j n_{j,x} + G_j n_{j,x} + \frac{1}{Re}\left[u_{,xx} + u_{,yy} + \Phi_{xx,x} + \Phi_{xy,y}\right] + \frac{1}{Fr^2}g_x, \tag{3}$$

$$v_t \;+\; uv_{,x} + vv_{,y} = -p_{,y} - w_{F,y} + R_j n_{j,y} + G_j n_{j,y} + \frac{1}{Re}\left[v_{,xx} + v_{,yy} + \Phi_{yx,x} + \Phi_{yy,y}\right] + \frac{1}{Fr^2}g_y. \tag{4}$$

$$\begin{aligned}\phi_t \;+\; u\phi_{,x} + v\phi_{,y} &= \frac{1}{Er\,\gamma_1}\left[\phi_{,xx} + \phi_{,yy}\right] - \frac{1}{2}(u_{,y} - v_{,x}) \\ &- \frac{1}{2}\frac{\gamma_2}{\gamma_1}\left[(u_{,y} + v_{,x})\cos(2\phi) + (v_{,y} - u_{,x})\sin(2\phi)\right] - \frac{1}{2}\frac{Re}{\gamma_1}\mu_0 \Delta\chi H^2 \sin(2(\phi_0 - \phi))\end{aligned} \tag{5}$$

where u_i is the velocity field, g_i is the gravitational field, $Re = \frac{\rho U L}{\eta}$ and $Er = UL\frac{\eta}{K}$ are the Reynolds and Ericksen numbers, respectively. For example, the term $R_j n_{j,x}$ is given by

$$\begin{aligned}R_j n_{j,x} = \frac{1}{Re}\Bigg\{ &- \gamma_1\phi_{,x}\left[\phi_{,t} + u\phi_{,x} \;+\; v\phi_{,y} + \frac{1}{2}(u_{,y} - v_{,x})\right] \\ &- \frac{1}{2}\left[\gamma_2\phi_{,x}\cos(2\phi)(u_{,y} + v_{,x}) + \gamma_2\phi_{,x}\sin(2\phi)(u_{,x} - v_{,y})\right]\Bigg\},\end{aligned} \tag{6}$$

and the function Φ_{ij}, called non-Newtonian stress tensor, hereafter, is given by

$$\Phi_{ij} = \alpha_1 n_k A_{kp} n_p n_i n_j + \alpha_2 N_i n_j + \alpha_3 n_i N_j + \alpha_5 n_j A_{ik} n_k + \; \alpha_6 n_i A_{jk} n_k\,. \tag{7}$$

In the equations above, the viscosities $\alpha_1, \ldots, \alpha_6$ have been scaled by a factor of $\eta = \frac{1}{2}\alpha_4$.

Equations (1), (3), (4) and Eq. (5) form the complete set of dynamic equations and must be solved subject to suitable boundary conditions in order to find solutions for u_i, p and ϕ, respectively.

2.2 Initial and Boundary Conditions

It is considered four types of boundaries: *prescribed inflows, outflows, rigid boundaries and moving free surfaces.* To solve equations (1), (3)–(4) and (5) it is necessary to impose boundary conditions for the velocity field on mesh boundaries. For rigid boundaries we employ the no-slip condition ($u_i = 0$) while at fluid entrances (inflows) the normal velocity is specified by $u_\nu = U_{inf}$ and the tangential velocities are set to zero, namely, $u_\mu = 0$, where ν denotes normal direction to the boundary and μ denotes tangential directions. At fluid exits (outflows) the Neumann condition $u_{i,\nu} = 0$ is employed.

On moving free surfaces, it is supposed that surface tension forces can be neglected so that the correct boundary conditions to be satisfied are (see (Batchelor, 1967)):

$$\boldsymbol{\nu}^T \cdot \mathbf{t} \cdot \boldsymbol{\nu} \;=\; 0, \tag{8}$$

$$\boldsymbol{\mu}^T \cdot \mathbf{t} \cdot \boldsymbol{\nu} \;=\; 0, \tag{9}$$

where $\boldsymbol{\nu}$ is the outward unit normal vector to the free surface and $\boldsymbol{\mu}$ is the unit tangential vector. The total stress tensor $\mathbf{t}$ is given by

$$t_{ij} = -p\delta_{ij} + \frac{1}{Re}\left[u_{i,j} + u_{j,i} + \Phi_{ij}\right] \tag{10}$$

For two-dimensional Cartesian flows, we take $\boldsymbol{\nu} = (\nu_x, \nu_y)^T$ and $\boldsymbol{\mu} = (-\nu_y, \nu_x)^T$ so that conditions (8) and (9) can be rewritten as

$$\widetilde{p} \;=\; \frac{2}{Re}\left[u_{,x}\nu_x^2 + v_{,y}\nu_y^2 + \nu_x\nu_y(u_{,y} + v_{,x})\right] + \frac{1}{Re}\left[\Phi^{xx}\nu_x^2 + \Phi^{yy}\nu_y^2 + \nu_x\nu_y(\Phi^{xy} + \Phi^{yx})\right] \tag{11}$$

$$0 \;=\; \frac{2}{Re}\left[(u_{,x} - v_{,y})\nu_x\nu_y + \frac{1}{2}\big(u_{,y} + v_{,x}\big)(\nu_y^2 - \nu_x^2)\right] + \frac{1}{Re}\left[\Phi^{xy}\nu_y^2 - \Phi^{yx}\nu_x^2 + \nu_x\nu_y(\Phi^{xx} - \Phi^{yy})\right]. \tag{12}$$

The boundary conditions for the orientation angle ϕ depends on the problem to be solved and will be especified in the sections dealing with numerical results.

3. GENSMAC-EL-MODEL2D

It is supposed that, at time t_n, the velocity field $u_i(x_k, t_n)$ and the orientation angle of the director $\phi(x_k, t_n)$ are known and that suitable boundary conditions are especified. The velocity field $u_i(x_k, t_{n+1})$, the pressure $p(x_k, t_{n+1})$, the non-Newtonian tensor $\Phi_{ij}(x_k, t_{n+1})$ and the orientation angle of the director $\phi(x_k, t_{n+1})$ are calculated by the following steps:

Step 1: Application of the free surface boundary conditions equations (11) and (12). In this step a pressure field $\widetilde{p}(x_k, t_n)$ that satisfies condition (12) is calculated. Also, condition (11) and the continuity equation are used to specify the velocities on the free surface. Details of these calculations are given in Section 4.1
Step 2: Using the values of $u_i(x_k, t_n)$ and $\phi(x_k, t_n)$, solve Eq. (2) for $w_F(x_k, t_n)$ and calculate $w_{F,i}(x_k, t_n)$ and then compute $\Phi_{ij}(x_k, t_n)$ from equations (7) and $R_j n_{j,i}(x_k, t_n), G_j n_{j,i}(x_k, t_n)$ from (6), respectively.
Step 3: Calculate an intermediate velocity field $\widetilde{u}_i(x_k, t_{n+1})$ by

$$\frac{\partial \widetilde{u}_i}{\partial t} = -(u_j\, u_i)_{,j} - \widetilde{p}_{,i} - w_{F,i} + R_j n_{j,i} + G_j n_{j,i} + \frac{1}{Re}\Big[(u_{i,j})_{,j} + \Phi_{ij,j}\Big] + \frac{1}{Fr^2} g_i\ , \tag{13}$$

with $\widetilde{u}_i(x_k, t_n) = u_i(x_k, t_n)$ and satifies the specified boundary conditions. It can be shown that $\widetilde{u}_i$ possesses the correct vorticity at time t_{n+1} (see (Tomé *et al.*, 1996)).

Step 4: Solve the Poisson equation

$$\psi_{,ii}(x_k, t_{n+1}) = \widetilde{u}_{i,i}(x_k, t_{n+1}) \tag{14}$$

subject to the boundary conditions: $\psi_{,\nu} = 0$ on rigid boundaries and inflows and $\psi = 0$ on free surfaces and outflows.

Step 5: Calculate the final velocity field

$$u_i(x_k, t_{n+1}) = \widetilde{u}_i(x_k, t_{n+1}) - \psi_{,i}(x_k, t_{n+1})\ . \tag{15}$$

It is easily verified that $u_{i,i}(x_k, t_{n+1}) = 0$.
Step 6: Compute the pressure field $p(x_k, t_{n+1})$ from (see (Tomé *et al.*, 1996))

$$p(x_k, t_{n+1}) = \widetilde{p}(x_k, t_n) + \frac{\psi(x_k, t_{n+1})}{\delta t}\ . \tag{16}$$

Step 7: By using $u_i(x_k, t_{n+1})$, solve equation (5) to obtain the angle of the director $\phi(x_k, t_{n+1})$.
Step 8: Calculate the components of the non-Newtonian tensor $\Phi_{ij}(x_k, t_{n+1})$ from equation (7).
Step 9: Fluid movement: The fluid is modeled by a list containing the coordinates of a set of marker-particles that defines its contour. The visualization of the fluid surface (and fluid's body) is obtained by connecting the particles by straight lines. This technique can cope with flows having multiple free surfaces that can colide with it other; it has been used for simulating Newtonian and viscoelastic free surface flows (e.g. (Tomé *et al.*, 2000, 2002)).

Thus, the last step in the calculation is to use the final velocity $u_i(x_k, t_{n+1})$ to move the marker-particles x_p to their new positions and to define the new fluid configuration. This is performed by solving

$$\frac{dx_p}{dt} = u_p(x_k, t_{n+1}), \tag{17}$$

where $u_p(x_k, t_{n+1})$ denotes the particle velocity that is calculated from a bilinear interpolation formula involving the four nearest grid velocities. After particle movement has been carried out it can happen that two particles may become too near to each other in which case may cause the storage of too many particles or two particles can be too far apart what is bad for the resolution of the free surface. To fix these irregularities, a procedure to delete and to insert particles, when necessary, is employed. A detailed discussion of the methodology employed to describe the fluid surface and particle movement is provided in Tomé *et al.* (2000).

4. FINITE DIFFERENCE APPROXIMATION

The equations contained in the numerical procedure outlined in the previous section will be solved by the finite difference method. For this type of grid the components of the non-Newtonian tensor $\Phi_{i,j}$, the pressure p, the density of elastic energy (2) and the angular momentum equation (5) are calculated at the centre of the computational cell $\big(i\delta x, j\delta y\big)$ while the velocity components u and v are calculated at the faces $\big((i+\frac{1}{2})\delta x, j\delta y\big)$ and $\big(i\delta x, (j+\frac{1}{2})\delta y\big)$, respectively. The time derivative in the momentum conservation equations (3)-(4) and in the angular momentum equation (5) are discretised by the explicit Euler method while the spatial derivatives are second order approximated.

Full details of the discretization employed for the equations in step 2. to step 8. have been provided in Cruz *et al.* (2013) and for reasons of space they are not presented here. However, in step 1, the equations dealing with the application of the free surface boundary conditions are presented in the next section.

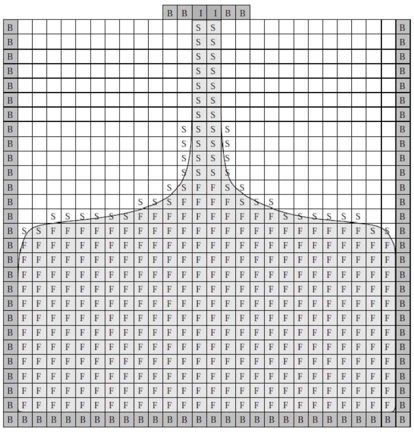

Figure 1: Illustration of cell type classification used.

Flows with moving surfaces are considered so that a scheme to identify the fluid region and the free surface is required. The scheme adopted herein classity the cells within the mesh as inflow cells (**I**), boundary cells (**B**), outflow cells (**O**), full cells (**F**), surface cells (**S**) and empty cells (**E**). Figure 1 displays an example of these cells for a given flow configuration. A detailed definition of theses types of cells can be found in Tomé *et al.* (1996).

4.1 Application of the free surface boundary conditions

Due to the presence of the Laplacian operator in the momentum and angular momentum equations (see equations (3), (4) and (5)), when calculating the velocities and the orientation angle on free surface cells (**S**), the values of these variables on empty cells (**E**) having one or more faces contiguous with S-cells are required. The values of theses variables can be assigned by using the mass conservation equation together with the surface stress conditions given by equations (11) and (12) according to three surface orientations, for reasons of space only one case is detailed here (for details see Tomé *et al.* (2002)):

Surface cells having one face contiguous with an E-cell: In these cells it is assumed that the free surface is either vertical or horizontal so that the unit normal vector takes the form $\boldsymbol{\nu} = (\pm 1,\ 0),$ or $\boldsymbol{\nu} = (0, \pm 1)$. For instance, if for the surface cell $\mathbf{S}_{i,j}$ the free surface is considered to be vertical, then we can take $\boldsymbol{\nu} = (1,0)$ in which case equations (11) and (12) yields

$$\widetilde{p} = \frac{1}{Re}\left[2\, u_{,x} + \Phi^{xx}\right], \tag{18}$$

$$-\frac{1}{Re}\left(u_{,y} + v_{,x} + \Phi^{yx}\right) = 0. \tag{19}$$

Also, mass conservation for the $\mathbf{S}_{i,j}$-cell gives $u_{,x} + v_{,y} = 0$.

The values of $\widetilde{p}_{i,j}, u_{i+1/2,j}, v_{i+1,j+1/2,j}$ and $\phi_{i+1,j}$ are required. They are obtained as follows: by discretizing the mass conservation at the cell centre (i,j) one obtains

$$\begin{cases} \dfrac{u_{i+\frac{1}{2},j} - u_{i-\frac{1}{2},j}}{\delta x} + \dfrac{v_{i,j+\frac{1}{2}} - v_{i,j-\frac{1}{2}}}{\delta y} = 0 \\ u_{i+\frac{1}{2},j} = u_{i-\frac{1}{2},j} - \dfrac{\delta x}{\delta y}(v_{i,j+\frac{1}{2}} - v_{i,j-\frac{1}{2}}). \end{cases} \tag{20}$$

The value of $v_{i+1,j+1/2,j}$ is calculated from (19) approximated at the cell corner $(i+\frac{1}{2}, j+\frac{1}{2})$ which gives

$$\begin{cases} \dfrac{u_{i+\frac{1}{2},j+1} - u_{i+\frac{1}{2},j}}{\delta y} + \dfrac{v_{i+1,j+\frac{1}{2}} - v_{i,j+\frac{1}{2}}}{\delta x} = \Phi^{yx}_{i+\frac{1}{2},j+\frac{1}{2}} \\ v_{i+1,j+\frac{1}{2}} = v_{i,j+\frac{1}{2}} - \frac{\delta x}{\delta y}(u_{i+\frac{1}{2},j+1} - u_{i+\frac{1}{2},j}) - \delta x \Phi^{yx}_{i+\frac{1}{2},j+\frac{1}{2}}. \end{cases} \tag{21}$$

After having calculated $u_{i+\frac{1}{2},j}$ by (20), the pressure $\widetilde{p}_{i,j}$ is computed from (18) discretized at the cell centre yielding

$$\widetilde{p}_{i,j} = \frac{1}{Re}\left[2\left(\frac{u_{i+\frac{1}{2},j} - u_{i-\frac{1}{2},j}}{\delta x}\right) + \Phi^{xx}_{ij}\right]. \tag{22}$$

The value of $\phi_{i+1,j}$ is obtained in order that $\frac{\partial \phi}{\partial x}|_{i+\frac{1}{2},j} = 0$ so that $\phi_{i+1,j} = \phi_{i,j}$. Other types of configuration of surface cells having one face contiguous with an E-cell the treatment for the application of the boundary conditions is similar.

5. VERIFICATION OF THE METHOD ON MOVING FREE SURFACE FLOWS

The finite difference equations discussed in Section 2. were implemented into the FREEFLOW2DNEMATIC code Cruz *et al.* (2013) in order to simulate free surface flows of LCP nematic fluids.

To show the convergence of the numerical method presented in this paper, the flow of a jet of diameter $D = 7$mm of a NEMATIC fluid impinging onto a rigid plate was simulated and mesh refinement studies were performed. A computational domain of size 13 cm $\times$ 13 cm was employed and the meshes used in these simulations were: M1: 91×91 (7 cells within the diameter of the jet); M2: 182×182(14 cells within the diameter of the jet) and M3: 364×364 (28 cells within the diameter of the jet). The remaining dat used are listed in Table 1. The properties of the fluid employed are shown in Table 2. The results of these simulations at times $t = 0.06$, 0.1 e 0.17s are presented in Fig. 2, where a good agreement between the solutions on the three meshes is displayed.

Table 1: Data used in the simulation of a jet impinging on a rigid plate.

U	D	H	H/D	Er	Re
1.0 ms^{-1}	7 mm	9 cm	12.86	1	1

Table 2: Nematic fluid model parameters used in Jet Impinging flow.

ρ	η	ν	K
1000 kg/m^3	7 Pa.s	0.007 m^2/s^2	0.049 N

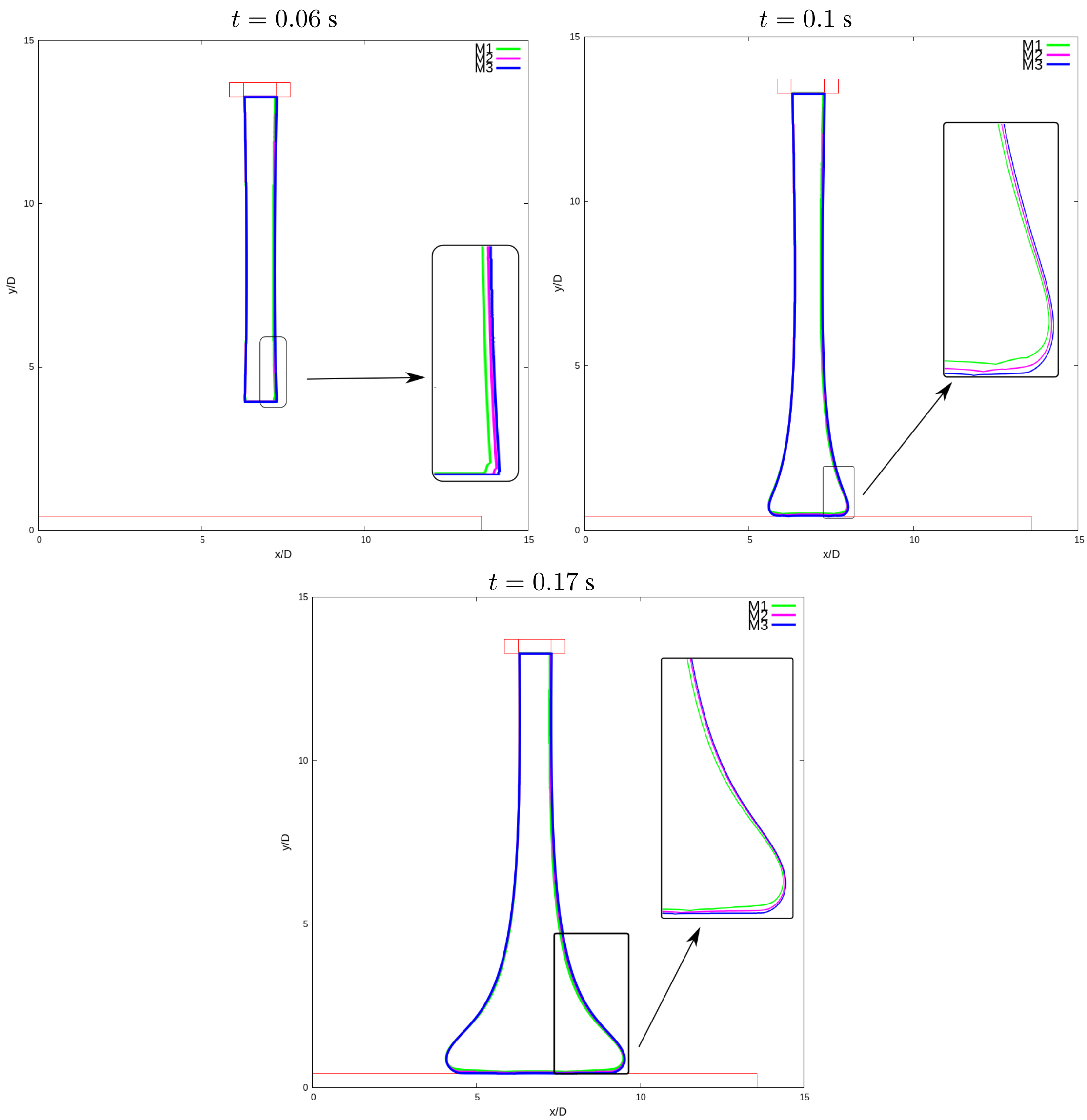

Figure 2: Fluid flow visualization at selected times on meshes M1, M2 and M3.

6. NUMERICAL SIMULATION OF NEMATIC LCPs FREE SURFACE FLOWS

In this section, a number of calculations performed by the computer code developed in this work on two-dimensional free surface flows of LCPs fluids are presented. The problems solved are common to several industrial applications, such as container filling and injection molding processes. Industries like food, chemical, among others, usually employ filling of containers in their production lines. The filling process is commonly carried out by a moving nozzle that injects the product in a fluid form into a container. During the filling stage, several problems can arise like splashing, jet buckling among others, and thus an understanding of the filling process are of valuable importance.

6.1 Numerical simulation of container filling

We present several calculation that simulate the filling of a square container of dimensions 4.0mm $\times 6.0$ mm. A centred inlet of diameter $D = 0.4$mm was positioned at the top of the container. The following input data were employed: $Re = 1$, $Fr = 3.033$, $Er = 1$. The scaling parameters were $U = 0.19$ m/s (fluid velocity at the nozzle), $D = 0.4$ mm (inlet diameter), $\rho = 1088$ and kinematic viscosity $\nu = 7.6 \times 10^{-5}$ m^2 s^{-1} ($\eta = 0.0826$ Pa.s). Gravity was assumed to be acting in the y-direction with $g_y = -9.81$ ms^{-2}. The elastic constant used for the calculus of the Ericksen numbers was $K = 6.3 \times 10^{-6}$ N. The mesh used in these simulations was 80×120 cells ($\delta x = \delta y = 0.05$ mm). On the container walls the no-slip condition was imposed while the director was anchored at walls so that the boundary conditions for ϕ was 0 on the bottom of the container and 90^o on the side walls.

The code solved this problem with the above input data. For comparison, the simulation with a Newtonian fluid ($Re = 1$) was also performed. Figures 3, 4, 5 and 6 displays a series of snapshots taken during these runs for LCP fluids with $Re = 1$ and $Er = 1$ and $Er = 5$.

The results displayed in Figs. 3, 4, 5 and 6 and 7 shows that the filling patterns for Newtonian and the LCP fluids with $Er = 1$ are not similar; for LCP fluids with $Er = 1$ we can observe a slight asymmetry in the flow, while the Newtonian fluid we observe that the flow is symmetric (see Fig. 7). We can see that the Newtonian jet and the jet LCP does not undergo buckling after flowing over the rigid plate. However, the LCP jet with $Er = 5$ starts to oscillate after reaching the rigid plate.

We believe that the viscoelastic jet exhibited with $Er = 5$ starts the buckling phenomenon because of elastic effects due to the increase in the Ericksen number.

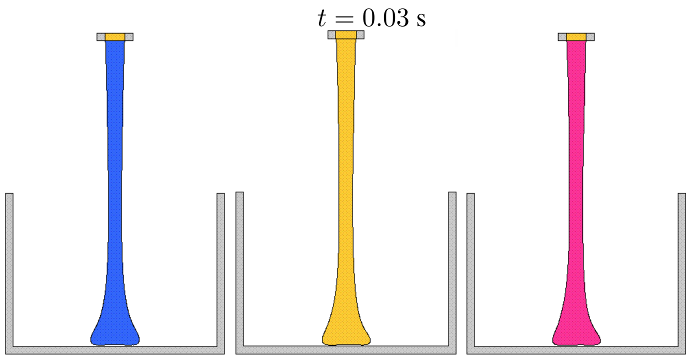

Figure 3: Numerical simulation of container filling. Newtonian flow (blue fluid – $Re = 1.0$) and Ericksen-Leslie Model Flow (yellow fluid – $Re = 1.0$-$Er = 1$ and pink fluid – $Re = 1.0$-$Er = 5$).

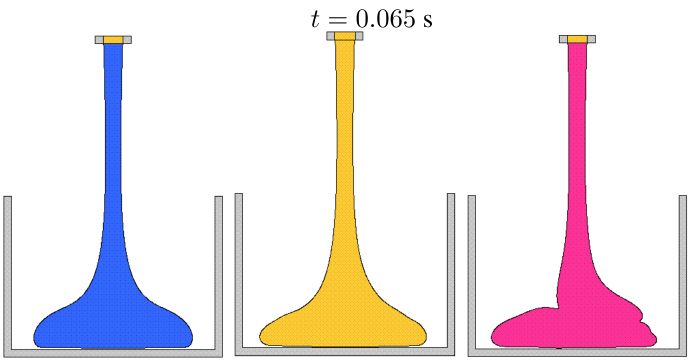

Figure 4: Numerical simulation of container filling. Newtonian flow (blue fluid – $Re = 1.0$) and Ericksen-Leslie Model Flow (yellow fluid – $Re = 1.0$-$Er = 1$ and pink fluid – $Re = 1.0$-$Er = 5$).

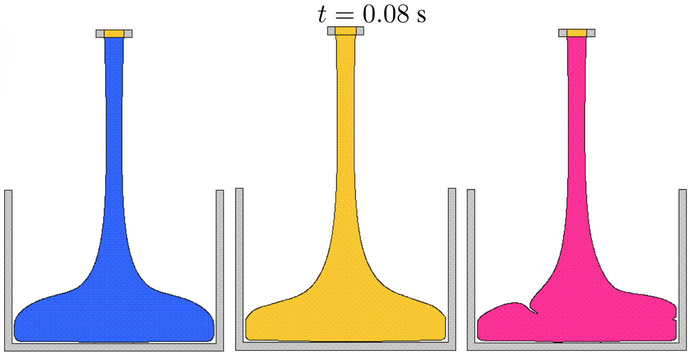

Figure 5: Numerical simulation of container filling. Newtonian flow (blue fluid – $Re = 1.0$) and Ericksen-Leslie Model Flow (yellow fluid – $Re = 1.0$-$Er = 1$ and pink fluid – $Re = 1.0$-$Er = 5$).

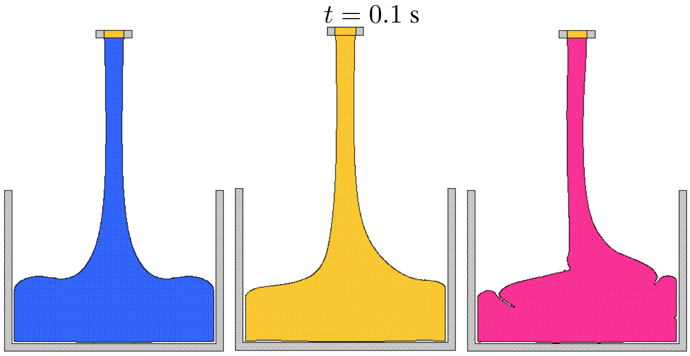

Figure 6: Numerical simulation of container filling. Newtonian flow (blue fluid – $Re = 1.0$) and Ericksen-Leslie Model Flow (yellow fluid – $Re = 1.0$-$Er = 1$ and pink fluid – $Re = 1.0$-$Er = 5$).

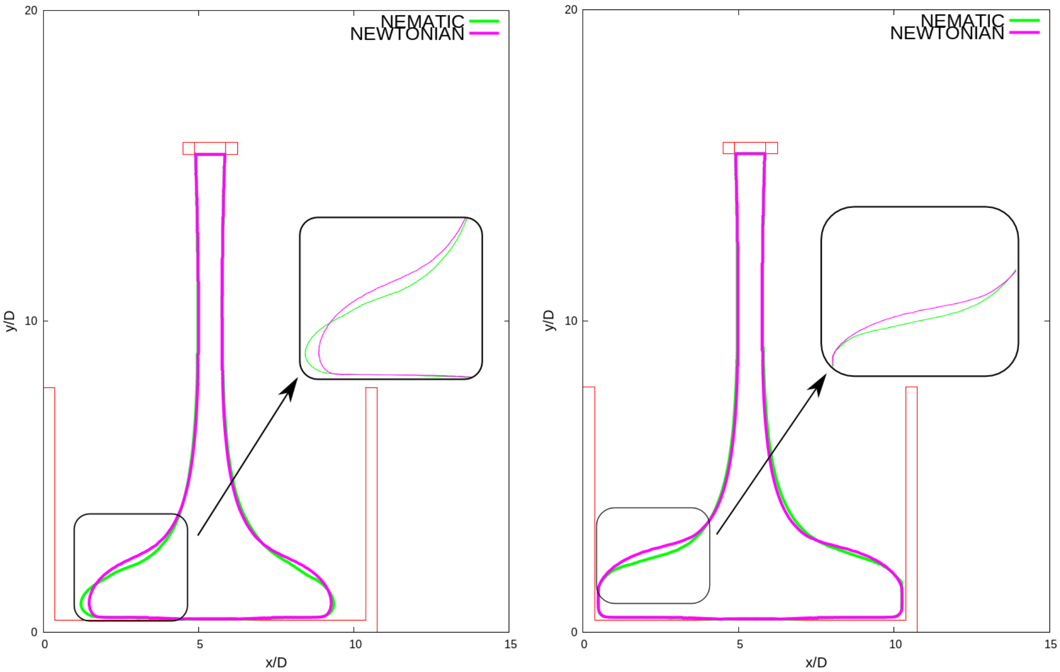

Figure 7: Development of the free surface at times $t = 0.065$ and 0.08 s. Newtonian flow - ($Re = 1.0$) and Ericksen-Leslie Model Flow - ($Re = 1.0$ and $Er = 1.0$).

7. CONCLUSIONS

This work presented a finite difference technique for simulating free surface flows of nematic liquid crystals modelled by the Ericksen-Leslie theory. We considered the free surface flow of a jet flowing onto a rigid plate. To verify the numerical technique this problem was simulated on three meshes and the results showed good agreement between the numerical solutions. Moreover, we simulated the jet flow problem using several Ericksen numbers. The results showed that the Ericksen-Leslie theory can also cope with elastic effects in free surface flows. In particular, it was shown that if the Ericksen number is large enough than a jet containing LCPs fluid can become unstable and exhibit the jet buckling phenomenon.

8. ACKNOWLEDGEMENTS

The authors would like to acknowledge the financial support given by the Brazilian funding agencies: FAPESP - Fundação de Amparo a pesquisa do Estado de São Paulo (grants 04/16064-9), CNPq - Conselho Nacional de Desenvolvimento Científico e Tecnológico (grants Nos. 470764/2007-4, 457373/2014-8, 306280/2014-0). This work is part of the activities developed within the CEPID-CeMEAI FAPESP project Grant No. $2013/07375-0$.

9. REFERENCES

Batchelor, G.K., 1967. *An Introduction to Fluid Dynamics*. Cambridge University Press, Cambridge.

Beaumont, J.P., Nagel, R. and Sherman, R., 2002. *Successful Injection Molding*. Hanser Publishers, Munich.

Bird, B., Armstrong, R.C. and Hassager, O., 1987. *Dynamics of Polymeric Liquids*. Wiley & Sons, New York.

Bociaga, E., 2001. *Processes determing the plastic flow in the injection mould and its efficiency*. Czestochowa University of Technology Publishers, Czestochowa.

Cruz, P.A., Tomé, M.F., Stewart, I.W. and McKee, S., 2010. "A numerical method for solving the dynamic three-dimensional ericksen-leslie equations for nematic liquid crystals subject to a strong magnetic field". *J. Non-Newtonian Fluid. Mech.*, Vol. 165, pp. 143–157.

Cruz, P.A., Tomé, M.F., Stewart, I.W. and McKee, S., 2011. "Numerical investigation of director orientation and flow of nematic liquid crystal in a planar 1:4 expansion". *Journal of Mechanics of Materials and Structures*, Vol. 6, pp. 1017–1030.

Cruz, P.A., Tomé, M.F., Stewart, I.W. and McKee, S., 2013. "Numerical solution of the ericksen-leslie dynamic equations for two-dimensional nematic liquid crystal flows". *Journal of Computational Physics*, Vol. 247, pp. 109–136.

Gonnet, J.M., Guillet, J., Raveyre, C., Assezat, G., Fulchiron, R. and Seytre, G., 2002. "In-line monitoring of the injection molding process by dielectric spectroscopy". *Polymer Engineering and Science*, Vol. 42, pp. 1171–1179.

Rey, A.D. and Denn, M.M., 2002. "Dynamical phenomena in liquid-crystalline materials". *Annu. Rev. Fluid Mech.*, Vol. 34, p. 233.

Smorawinski, A., 1989. *Injection moulding technology*. WNT, Warsaw.

Tomé, M.F., Castelo, A., Murakami, J., Cuminato, J.A., Minghim, R., oliveira, M.C.F., Mangiavacchi, N. and McKee, S., 2000. "Numerical simulation of axisymmetric free surface flows". *J. Comput. Phys.*, Vol. 157, pp. 441–472.

Tomé, M.F., Duffy, B. and McKee, S., 1996. "A numerical technique for solving unsteady non-newtonian free surface flows". *J. Non-Newtonian Fluid Mech.*, Vol. 62, pp. 9–34.

Tomé, M.F., Mangiavacchi, N., Cuminato, J.A., Castelo, A. and McKee, S., 2002. "A numerical technique for solving unsteady non-newtonian free surface flows". *J. Non-Newtonian Fluid Mech.*, Vol. 106, pp. 61–106.

10. RESPONSIBILITY NOTICE